

# Template-assisted synthesis of $\text{PbTiO}_3$ nanotubes

Per Martin Rørvik<sup>a</sup>, Kiyoharu Tadanaga<sup>b</sup>, Masahiro Tatsumisago<sup>b</sup>,  
Tor Grande<sup>a</sup>, Mari-Ann Einarsrud<sup>a,\*</sup>

<sup>a</sup> Department of Materials Science and Engineering, Norwegian University of Science and Technology, 7491 Trondheim, Norway

<sup>b</sup> Department of Applied Chemistry, Graduate School of Engineering, Osaka Prefecture University, Sakai, Osaka 599-8531, Japan

Received 5 November 2008; received in revised form 6 February 2009; accepted 12 February 2009

Available online 14 March 2009

## Abstract

Nanotubes of ferroelectric lead titanate ( $\text{PbTiO}_3$ ) have been made by a template-assisted method. An equimolar Pb–Ti sol was dropped onto porous alumina membranes and penetrated into the channels of the template. Single-phase  $\text{PbTiO}_3$  perovskite nanotubes were obtained by annealing at 700 °C for 6 h. The nanotubes had diameters of 200–400 nm with a wall thickness of approximately 20 nm. Excess PbO or annealing in a Pb-containing atmosphere was not necessary in order to achieve single-phase  $\text{PbTiO}_3$  nanotubes. The influence of the heating procedure and the sol concentration is discussed.

© 2009 Elsevier Ltd. All rights reserved.

**Keywords:** Powders-chemical preparation; Sol–gel processes; Nanotubes; Perovskites;  $\text{PbTiO}_3$

## 1. Introduction

Template-assisted synthesis is a widely used method to produce one-dimensional (1D) nanostructures such as nanotubes and nanowires of a variety of materials.<sup>1</sup> For oxide materials, the most commonly used negative templates are porous anodic aluminium oxide (AAO) and track-etched polycarbonate membranes.<sup>2</sup> These templates have 1D pores or channels in which a sol or an aqueous solution containing the desired components can be incorporated. In following drying and annealing steps, the solvent evaporates and the material starts to crystallize and densify, forming nanostructures with dimensions constricted by the pore diameter and the pore length of the template.

In this work we used commercial Whatman Anodisc AAO membranes to synthesize  $\text{PbTiO}_3$  nanotubes.  $\text{PbTiO}_3$  is a prototype ferroelectric material with a perovskite structure and with a Curie temperature of 490 °C.  $\text{PbTiO}_3$  has previously been synthesized in AAO templates, producing nanotubes by sol–gel method<sup>3–6</sup> and nanowires by an aqueous solution method.<sup>7</sup> In addition, the closely related compound  $\text{PbZr}_{1-x}\text{Ti}_x\text{O}_3$  (PZT) has also been synthesized as nanotubes and nanowires in AAO

templates.<sup>8–15</sup>  $\text{PbTiO}_3$  nanotubes are interesting for instance in fundamental studies of nanoscale ferroelectricity, in non-volatile memory applications,<sup>9,14</sup> and in piezoelectric applications.<sup>9</sup> In this work we studied how the heating procedure, the sol concentration, and different nominal pore diameters of the Anodisc membranes influenced the morphology and the phase composition of the nanotubes.

## 2. Experimental

Whatman Anodisc AAO membranes with a thickness of 60  $\mu\text{m}$  were used as templates. Three types of membranes with different nominal pore diameters were used: 20, 100, and 200 nm. The diameter of the membrane was either 25 mm (200 nm membranes) or 47 mm (20 and 100 nm membranes). The pore diameters on the two sides of the membrane were different. For instance, the small pore side of the 200 nm Anodisc membranes had pore diameters  $\leq 100$  nm, while the large pore side had pore diameters of 200–250 nm (Fig. 1). The pore diameter across the membrane was therefore inhomogeneous.

A Pb–Ti sol was made by dissolving lead(II) acetate trihydrate (Wako, >99.9%) in acetic acid (Wako, >99.0%), and titanium(IV) tetrabutoxide (Wako, >95.0%) in 2-methoxyethanol (Wako, >98.0%), and mixing these two solutions by stirring. Three sol concentrations were used: 0.43, 0.75 and 1.35 mol/L

\* Corresponding author. Tel.: +47 73594002.

E-mail address: [mari-ann.einarsrud@material.ntnu.no](mailto:mari-ann.einarsrud@material.ntnu.no) (M.-A. Einarsrud).

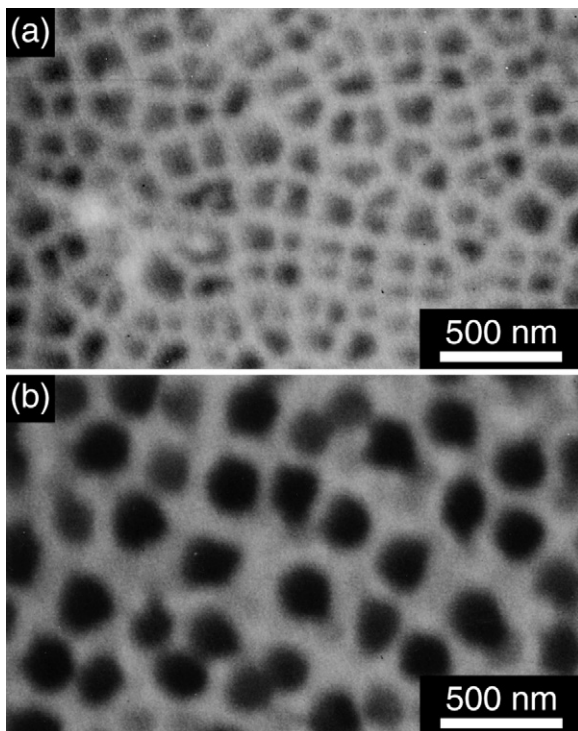


Fig. 1. SEM images of a Whatman Anodisc membrane with 200 nm nominal pore diameter. (a) Small pore side. (b) Large pore side.

( $n_{\text{Pb}}/V_{\text{total}}$ ), see Table 1. The Pb/Ti ratio was 1.00 for all the sols. The sol was dropped onto the large pore side of a membrane which had been taped at the small pore side. After 10 min, excess sol was removed by wiping with a paper or with a scalpel. The membranes infiltrated with the sol were dried in air for 30 min and thereafter heat-treated at 700 °C for 0.5–6 h. The membranes were either directly heated to 700 °C in a preheated furnace, or slowly heated at a rate of 1 °C/min from room temperature. The cooling rate was 3 °C/min for all the experiments. After the heat treatment, excess  $\text{PbTiO}_3$  material was carefully scraped off using a scalpel. The membrane was dissolved by immersing in 4 mol/L NaOH for at least 1 h, followed by washing and centrifugation in water. Large-area arrays of nanotubes were obtained by coating the small pore side of the membrane with epoxy before the NaOH treatment, while free-standing nanotubes were obtained by sonication during the NaOH treatment. For comparison, the sols were also heat-treated, at 700 °C for 0.5 h with a 1 °C/min heating rate.

The phase composition of the products was studied by X-ray powder diffraction (XRD, Shimadzu LabX XRD-6000). The morphology of the products and the Anodisc membranes

Table 1  
Amount of reactants and sol concentration for the three different sols used.

Sol number	1	2	3
Cation concentration	0.43 mol/L	0.75 mol/L	1.35 mol/L
Lead(II) acetate trihydrate	10.0 mmol	10.0 mmol	10.0 mmol
Titanium(IV) tetrabutoxide	10.0 mmol	10.0 mmol	10.0 mmol
Acetic acid	2.0 mL	5.0 mL	10.0 mL
2-Methoxyethanol	2.0 mL	5.0 mL	10.0 mL

was studied by scanning electron microscopy (SEM, JEOL JSM-5300), and field emission scanning electron microscopy (FESEM, Hitachi S-4500). The samples were coated with gold or osmium before imaging.

### 3. Results

The diameters of nanotubes synthesized in 200 nm membranes were 200–400 nm, while the lengths varied from 2  $\mu\text{m}$  to above 10  $\mu\text{m}$  (Fig. 2). A side view of the nanotube array shows that the growth of nanotubes was inhomogeneous in the membrane (Fig. 2b), suggesting that the internal structure of the membrane was inhomogeneous. During the drying after dissolving the membrane the nanotubes typically bundled together (Fig. 2c). However, the nanotubes could detach from each other easily by sonication (Fig. 2d).

The X-ray diffractograms of the heat-treated products show that while the perovskite phase ( $\text{PbTiO}_3$ ) was formed from the sol after annealing at 700 °C for 30 min with slow heating rate (Fig. 3a), the same heat treatment for the sol in the membrane resulted in the metastable fluorite phase (Fig. 3b),<sup>16,17</sup> which is non-ferroelectric and therefore unwanted. Prolonged heating increased the perovskite content (Fig. 3c); however, it was more effective to insert the sol-infiltrated membrane directly into a furnace preheated to 700 °C (Fig. 3d–f). Initially, a small amount of the fluorite phase was formed also with the direct heating, but after 6 h at 700 °C the fluorite phase could not be detected by XRD (Fig. 3f).

Comparing Fig. 3f with a, the diffraction lines in Fig. 3f are much broader than the corresponding lines in Fig. 3a, and in addition the splitting of the (1 0 1) and (1 1 0) diffraction lines at 32–33° evident in Fig. 3a is far less pronounced in Fig. 3f. The difference between these two diffractograms is caused by line broadening because of small crystallite sizes. Similar diffractograms to Fig. 3f have been shown for  $\text{PbTiO}_3$  nanotubes that exhibited ferroelectric properties, implying a tetragonal structure.<sup>6</sup> The line broadening indicates that the perovskite crystallites formed in the membrane are much smaller than the crystallites formed during heat treatment of the sol. The template therefore has a confinement effect on the coalescence of the nanoparticles.

To study if the wall thickness of the nanotubes could be controlled by changing the sol concentration, three different sols (Table 1) were used with otherwise identical synthesis conditions. However, the wall thickness estimated from FESEM images was 15–20 nm for all the three sol concentrations and no significant difference was observed (Fig. 4). Fig. 4 also shows that the nanotubes were polycrystalline, consisting of grains with diameters  $\leq 20$  nm.

Anodisc membranes with 20 and 100 nm nominal pore diameters were tried used to make  $\text{PbTiO}_3$  nanotubes with smaller diameter. However, the nanotube diameters were the same as when the 200 nm membranes were used; 200–400 nm. Cross-section SEM images of a 100 nm membrane show that it was only a thin layer ( $\sim 1.5 \mu\text{m}$ ) at the small pore side of the membrane that had the nominal pore diameter, while the rest of the membrane had larger pores (200–400 nm) (Fig. 5). The layer

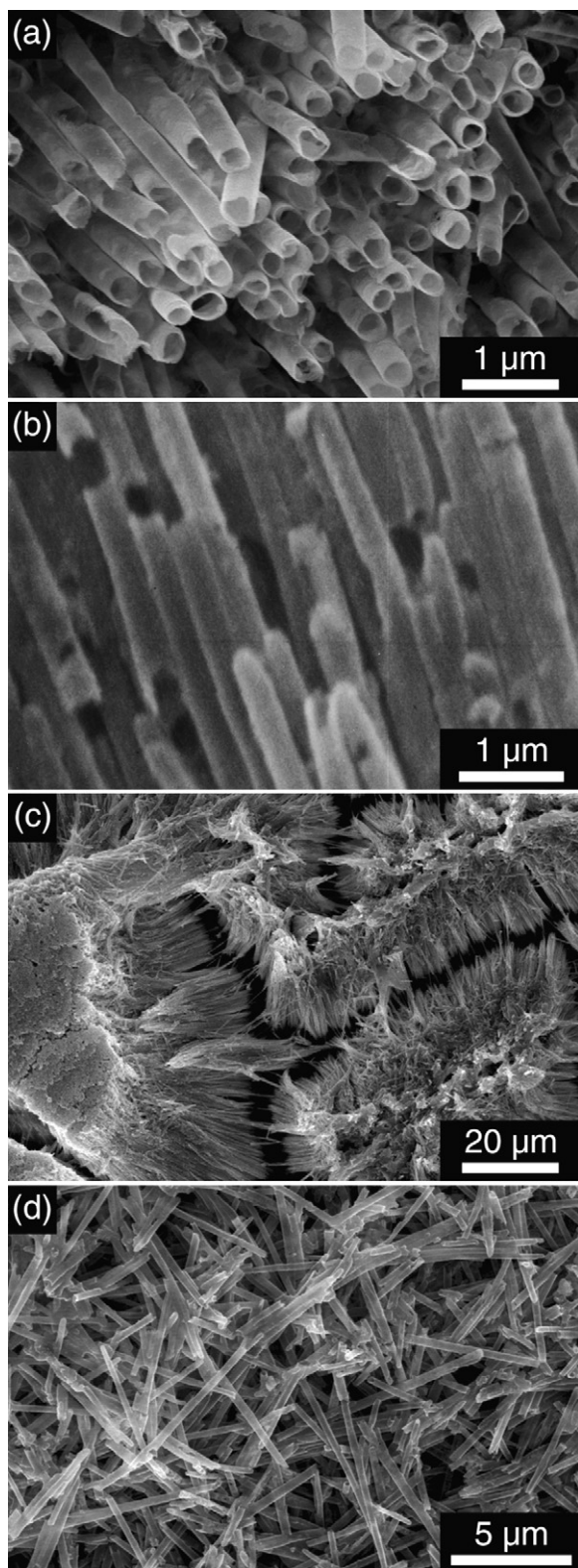


Fig. 2. SEM and FESEM images of nanotubes synthesized in 200 nm membranes. (a) Nanotube ends. (b) Side view revealing growth inhomogeneities. (c) The nanotubes bundled during drying after dissolving the membrane. (d) Free-standing nanotubes after sonication.

with small pore diameter in the 20 nm membranes was even thinner ( $<1 \mu\text{m}$ ).

#### 4. Discussion

The results show that template-assisted synthesis is an easy method to fabricate ceramic nanotubes. However, control of the micro/nanostructure and phase composition can be a challenge. For the  $\text{PbTiO}_3$  system studied here, the effect of various heat treatment procedures on the resulting phase is clearly demonstrated in Fig. 3. The non-ferroelectric fluorite phase that was formed during slow heating of the membranes is often

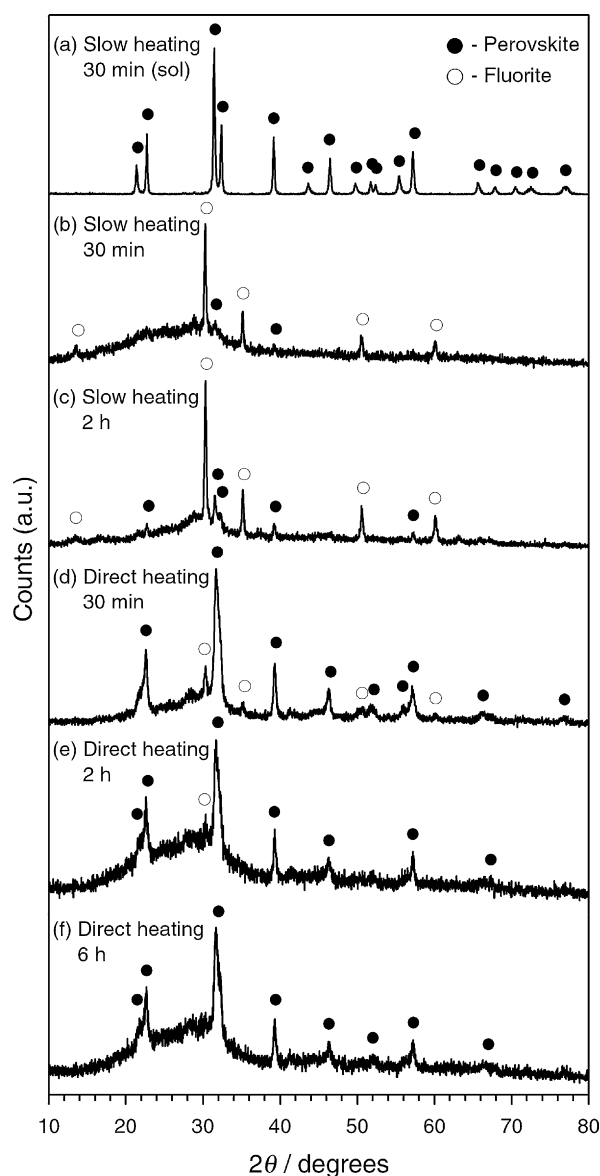


Fig. 3. X-ray diffractograms of products synthesized with 0.75 mol/L sol after various heat treatments. (a) Sol annealed at 700 °C for 30 min with slow heating rate (1 °C/min). (b)–(f) Products synthesized in 200 nm membranes (the membranes were dissolved before XRD characterization). The products were annealed at 700 °C for the stated length of time, and were either slowly heated (1 °C/min) to 700 °C, or directly inserted into a furnace preheated to 700 °C. Line identities are based on the PDF standard patterns of tetragonal perovskite  $\text{PbTiO}_3$  (6-452) and pyrochlore  $\text{Pb}_2\text{Ti}_2\text{O}_6$  (26-142).



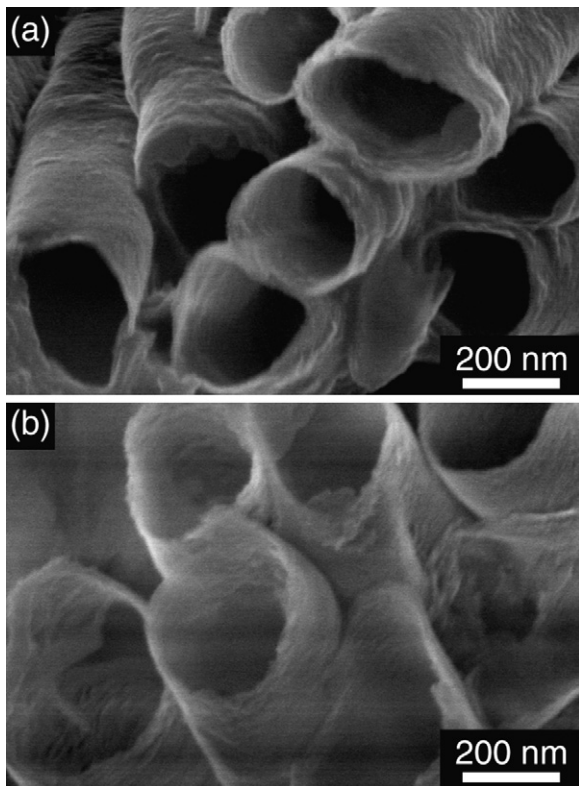


Fig. 4. FESEM images of nanotubes synthesized in 200 nm membranes using sol concentrations of (a) 0.43 mol/L and (b) 1.35 mol/L.

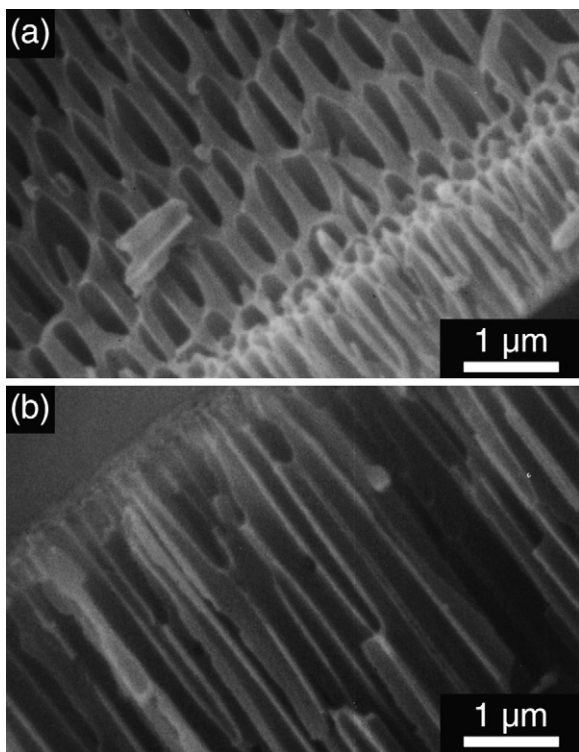


Fig. 5. SEM images of the cross-section of a Whatman Anodisc membrane with 100 nm nominal pore diameter. (a) Small pore side. (b) Large pore side.

encountered as an unwanted intermediate phase during annealing of Pb-based ferroelectrics.<sup>17–20</sup> In the fluorite structure, neither the oxygen vacancies nor the cations are ordered, so during annealing, formation of the metastable fluorite phase may be kinetically favoured over the thermodynamically stable, but highly ordered perovskite phase, because of limited ion diffusion at lower temperatures.<sup>17,18</sup> The formation of the fluorite phase will also reduce the driving force associated with the nucleation of the perovskite phase.<sup>18</sup> Thus, when the fluorite phase is nucleated from the amorphous precursor, the further transformation into the perovskite phase is slow, although the perovskite phase is the thermodynamically stable phase. The difference in phase composition between the powders that were obtained by the slow heat treatment of the sol (Fig. 3a) and the sol in the membrane (Fig. 3b), indicates that the pore walls of the membrane influence the nucleation and growth process. As the fluorite phase was only observed in the diffractogram of the membrane-synthesized sample (Fig. 3b), it can be assumed that heterogeneous nucleation of the fluorite phase occurred at the pore walls, in a temperature range in which the fluorite phase is kinetically stable. In contrast, for the sol alone, homogeneous nucleation is more likely, and the homogeneous nucleation is likely to be initiated at a higher temperature than the heterogeneous nucleation. At this higher temperature, the perovskite phase may be the preferred phase, so that in absence of the membrane, the perovskite phase is formed because heterogeneous nucleation is less likely.

Further, the direct heating procedure, in which the membrane was inserted into a preheated furnace, promotes nucleation of the perovskite phase because the rapid thermal processing bypasses the temperature range where the fluorite phase is kinetically stable. A small fraction of the fluorite phase was formed also during the direct heating procedure; however, by prolonged annealing time at 700 °C (up to 6 h) the fluorite phase transformed into the perovskite phase (Fig. 3d–f). The fluorite phase has a much higher tolerance for Pb deficiency than the perovskite phase,<sup>18</sup> so the complete transformation of the fluorite phase into the perovskite phase also shows that significant volatilization of Pb did not occur, although the precursor solution had a 1.00 Pb/Ti ratio and the nanotubes have a high surface/volume ratio. A standard approach to compensate for Pb loss during annealing of Pb-based ferroelectrics is addition of 5–25 mol% excess Pb to the precursor solution, or annealing in a Pb- or PbO-rich atmosphere.<sup>18</sup> In the previous reports of PbTiO<sub>3</sub> nanotubes made by sol-gel processing in AAO membranes, either a Pb/Ti ratio of 1.05 was used<sup>4,6</sup> or not specified,<sup>3</sup> or the annealing was performed in a Pb vapour-saturated atmosphere.<sup>5</sup> In contrast, this study shows that single-phase perovskite nanotubes can be obtained with an equimolar precursor solution, provided that a direct heating procedure is used during the annealing. Excessive lead is generally unwanted as it can diffuse into Pt electrodes and decrease the dielectric constant and the resistivity.<sup>20</sup>

The concentration of the sol did not significantly influence the morphology of the nanotubes (Fig. 4). This has also been reported by Hernandez-Sanchez et al.<sup>4</sup> Although the 1.35 mol/L sol was three times as concentrated as the 0.43 mol/L sol, the wall thicknesses estimated from the FESEM images were the

same (15–20 nm). It may be that the difference is too small to be observable by FESEM. A possible explanation for the equal wall thickness is that the higher viscosity of the high concentration sol lowers the ability of the sol to penetrate the pores, especially for the long pores used here (60  $\mu\text{m}$ ), thus reducing the amount of material that is deposited in the pores. The wall thickness is most importantly affected by the pore diameter, as Zhao et al.<sup>5</sup> have shown that the wall thickness increased with the diameter of the nanotubes. From the results of Zhao et al., a wall thickness of 10–15% of the pore diameter is expected, which is consistent with the 20 nm wall thickness obtained in the 200 nm pore diameter membranes in the present study. To increase the wall thickness, successive coatings of the template can be used, but the fragile nature of the AAO membranes makes such a procedure difficult.<sup>4</sup> Increasing the immersion time can also be an alternative, as Zhang et al.<sup>10</sup> reported the synthesis of PZT nanowires in a 45 nm AAO membrane using a long sol immersion time of 5 h. However, to synthesize  $\text{PbTiO}_3$  or PZT nanowires instead of nanotubes in AAO membranes, growth by a particle-directing method such as electrophoresis<sup>21</sup> or growth from aqueous salt solutions<sup>7</sup> is probably more suitable.

The commercial membranes that were used in this work have most likely been produced by a one-step procedure, in which the aluminium film has only been anodized once. By a two-step procedure, a much better control of the pore diameter and pore distribution can be obtained, with a constant pore diameter throughout the membrane.<sup>22</sup> Therefore, to make nanotubes with diameters below 200 nm, it is necessary with a more careful preparation of the membrane templates.

## 5. Conclusions

$\text{PbTiO}_3$  nanotubes with diameters of 200–400 nm were successfully prepared by a template-assisted method. Direct heating at 700 °C for 6 h was shown to be sufficient to obtain single-phase perovskite nanotubes from an equimolar precursor solution, avoiding the addition of excess lead or annealing in a Pb-rich atmosphere. Variation of the sol concentration did not significantly affect the wall thickness of the nanotubes. Large internal pores in the Anodisc membranes with nominal pore diameters of 20 and 100 nm prevented the formation of nanotubes with smaller diameters.

## Acknowledgements

A research stay at Osaka Prefecture University for Per Martin Rørvik was financially supported by the International Section at the Norwegian University of Science and Technology (NTNU) and the Scandinavia-Japan Sasakawa Foundation. This work was additionally financially supported by the Strategic Area of Materials at NTNU.

## References

- Cao, G. and Liu, D., Template-based synthesis of nanorod, nanowire, and nanotube arrays. *Adv. Colloid Interface*, 2008, **136**, 45–64.
- Bae, C., Yoo, H., Kim, S., Lee, K., Kim, J., Sung, M. M. et al., Template-directed synthesis of oxide nanotubes: fabrication, characterization, and applications. *Chem. Mater.*, 2008, **20**, 756–767.
- Hernandez, B. A., Chang, K.-S., Fischer, E. R. and Dorhout, P. K., Sol-gel template synthesis and characterization of  $\text{BaTiO}_3$  and  $\text{PbTiO}_3$  nanotubes. *Chem. Mater.*, 2002, **14**, 480–482.
- Hernandez-Sanchez, B. A., Chang, K.-S., Scancelli, M. T., Burris, J. L., Kohli, S., Fischer, E. R. et al., Examination of size-induced ferroelectric phase transitions in template synthesized  $\text{PbTiO}_3$  nanotubes and nanofibers. *Chem. Mater.*, 2005, **17**, 5909–5919.
- Zhao, L., Steinhart, M., Yu, J. and Gösele, U., Lead titanate nano- and microtubes. *J. Mater. Res.*, 2006, **21**, 685–690.
- Liu, L., Ning, T., Ren, Y., Sun, Z., Wang, F., Zhou, W. et al., Synthesis, characterization, photoluminescence and ferroelectric properties of  $\text{PbTiO}_3$  nanotube arrays. *Mater. Sci. Eng. B*, 2008, **149**, 41–46.
- Hsu, M. C., Leu, I. C., Sun, Y. M. and Hon, M. H., Template synthesis and characterization of  $\text{PbTiO}_3$  nanowire arrays from aqueous solution. *J. Solid State Chem.*, 2006, **179**, 1421–1425.
- Luo, Y., Szafraniak, I., Zakharov, N. D., Nagarajan, V., Steinhart, M., Wehrspohn, R. B. et al., Nanoshell tubes of ferroelectric lead zirconate titanate and barium titanate. *Appl. Phys. Lett.*, 2003, **83**, 440–442.
- Morrison, F. D., Luo, Y., Szafraniak, I., Nagarajan, V., Wehrspohn, R. B., Steinhart, M. et al., Ferroelectric nanotubes. *Rev. Adv. Mater. Sci.*, 2003, **4**, 114–122.
- Zhang, X. Y., Zhao, X., Lai, C. W., Wang, J., Tang, X. G. and Dai, J. Y., Synthesis and piezoresponse of highly ordered  $\text{Pb}(\text{Zr}_{0.53}\text{Ti}_{0.47})\text{O}_3$  nanowire arrays. *Appl. Phys. Lett.*, 2004, **85**, 4190–4192.
- Zhigalina, O. M., Mishina, E. D., Sherstyuk, N. E., Vorotilov, K. A., Vasiljev, V. A., Sigov, A. S. et al., Crystallization of PZT in porous alumina membrane channels. *Ferroelectrics*, 2006, **336**, 247–254.
- Liu, M., Li, X., Imrane, H., Chen, Y., Goodrich, T., Cai, Z. et al., Synthesis of ordered arrays of multiferroic  $\text{NiFe}_2\text{O}_4$ – $\text{Pb}(\text{Zr}_{0.52}\text{Ti}_{0.48})\text{O}_3$  core-shell nanowires. *Appl. Phys. Lett.*, 2007, **90**, 152501.
- Yang, S. A., Jeong, K. O., Kim, J., Choi, Y. C., Han, J. K. and Bu, S. D., Synthesis of PZT nanotubes and its nanometer-scale shape modification with an electron-beam irradiation. *J. Korean Phys. Soc.*, 2007, **51**, S174–S177.
- Kim, J., Yang, S. A., Choi, Y. C., Han, J. K., Jeong, K. O., Yun, Y. J. et al., Ferroelectricity in highly ordered arrays of ultra-thin-walled  $\text{Pb}(\text{Zr,Ti})\text{O}_3$  nanotubes composed of nanometer-sized perovskite crystallites. *Nano Lett.*, 2008, **8**, 1813–1818.
- Nourmohammadi, A., Bahrevar, M. A., Schulze, S. and Hietschold, M., Electrodeposition of lead zirconate titanate nanotubes. *J. Mater. Sci.*, 2008, **43**, 4753–4759.
- The oxygen-deficient fluorite and pyrochlore structures are closely related for the phases of interest here ( $\text{Pb}_2\text{Ti}_2\text{O}_6$ ). The defining difference between the two phases is the presence (pyrochlore) or absence (fluorite) of cationic ordering.<sup>17</sup> Such ordering is beyond the scope of the present study, and we will therefore refer to the non-ferroelectric metastable phase as “fluorite”.
- Polli, A. D., Lange, F. F. and Levi, C. G., Metastability of the fluorite, pyrochlore, and perovskite structures in the  $\text{PbO}$ – $\text{ZrO}_2$ – $\text{TiO}_2$  system. *J. Am. Ceram. Soc.*, 2000, **83**, 873–881.
- Lefevre, M. J., Speck, J. S., Schwartz, R. W., Dimos, D. and Lockwood, S. J., Microstructural development in sol-gel derived lead zirconate titanate thin films: the role of precursor stoichiometry and processing environment. *J. Mater. Res.*, 1996, **11**, 2076–2084.
- Schwartz, R. W., Chemical solution deposition of perovskite thin films. *Chem. Mater.*, 1997, **9**, 2325–2340.
- Brennecka, G. L., Parish, C. M., Tuttle, B. A., Brewer, L. N. and Rodriguez, M. A., Reversibility of the perovskite-to-fluorite phase transformation in lead-based thin and ultrathin films. *Adv. Mater.*, 2008, **20**, 1407–1411.
- Limmer, S. J., Seraji, S., Forbess, M. J., Wu, Y., Chou, T. P., Nguyen, C. et al., Electrophoretic growth of lead zirconate titanate nanorods. *Adv. Mater.*, 2001, **13**, 1269–1272.
- Li, A. P., Müller, F., Birner, A., Nielsch, K. and Gösele, U., Polycrystalline nanopore arrays with hexagonal ordering on aluminum. *J. Vac. Sci. Technol. A*, 1999, **17**, 1428–1431.